Compositional Thresholds and Anomalies in Connection with Stiffness Transitions in Network Glasses

M. Bauchy,[1] M. Micoulaut,[1,*] M. Boero,[2] and C. Massobrio[2]

[1]*Laboratoire de Physique Théorique de la Matière Condensée, Université Pierre et Marie Curie, 4 Place Jussieu, F-75252 Paris Cedex 05, France*

[2]*Institut de Physique et de Chimie des Matériaux de Strasbourg, University of Strasbourg-CNRS UMR 7504, 23 rue du Loess, F-67034 Strasbourg Cedex 2, France*

(Received 26 November 2012; published 15 April 2013)

The structural and dynamical properties of amorphous and liquid As_xSe_{1-x} ($0.2 < x < 0.4$) are studied by first principles molecular dynamics. Within the above range of compositions, thresholds and anomalies are found in the behavior of reciprocal space properties that can be correlated to the experimental location of the so-called Boolchand intermediate phase in these glassy networks. These findings are associated with diffusion anomalies for the parent liquid phase, thereby linking structural and dynamical atomic-scale fingerprints for the onset of rigidity within the network, while also providing a much more complex picture than the one derived from mean-field approaches of stiffness transitions.

DOI: 10.1103/PhysRevLett.110.165501 PACS numbers: 61.43.Fs, 71.15.Pd, 72.80.Ng

Network-forming glasses are characterized by a threshold which marks a transition in their physical properties. This threshold is the consequence of structural modifications which increase the overall network connectivity. Such topological changes, induced by composition, drive the structure from a flexible phase containing local deformation (floppy) modes to a stressed rigid phase. Within the framework of rigidity theory, inspired by the early work of Maxwell, one can associate n_c constraints to stretching and bonding interatomic forces [1,2]. When n_c equals the number of degrees of freedom per atom, networks are isostatic and fulfill exactly the Maxwell stability criterion. In glasses, this particular situation has been identified as a stiffness transition at a network mean coordination number $\bar{r} = 2.4$ [1,3]. Chalcogenide glasses (e.g., A_xSe_{1-x} with $A =$ Ge, As) have served for this reason as benchmark systems because their network mean coordination number $\bar{r}$ can be tuned rather easily with changing composition. Recent applications of these concepts led to the design of new material functionalities stemming from the flexible or rigid nature of the underlying networks [4–8].

In the search for structural signatures of the rigidity transition, the presence of anomalies in measured reciprocal space properties is expected to provide unambiguous clues. However, measurements of the total neutron or x-ray structure factor $S_T(k)$ did not lead to any compelling evidence of structural patterns underlying a specific transition [9–11]. This is true both for threshold behaviors at a given concentration and for changes occurring in a finite concentration range, as those characterizing the so-called *intermediate phase* (IP) determined by Boolchand and coworkers [12]. Despite recent combined experimental and modeling efforts, the occurrence of unambiguous structural marks of the rigidity transition and/or the IP phase remains an elusive issue [13].

In this Letter we show that a certain number of anomalies in structural properties take place in some measurable structural properties (partial structure factors, pair distribution functions) of As_xSe_{1-x} glasses. Our assertion is based on first-principles molecular dynamics data of an As-Se model with changing composition. We show that the characteristic parameters of the first sharp diffraction peak (FSDP) in the partial structure factor $S_{AsSe}(k)$ display a threshold and a minimum for the peak position and peak width, respectively. Such structural signatures should be detected from isotopic substituted neutron diffraction allowing access to the partial structure factors. In real space, the onset of rigidity is tightly linked with an important increase of homopolar As-As bonds. These findings can be correlated with diffusivity anomalies in the supercooled liquid which manifest by a maximum and a minimum at a composition $As_{35}Se_{65}$ in the self-diffusion constants and diffusion activation energies, respectively. The compositional locations of these anomalies correspond to the experimentally determined intermediate phase compositions. While no double transition that could serve to define an IP is found, we establish a clear correlation between anomalies in MD-calculated properties and those determined experimentally [14] in the IP. Furthermore, complex atomic scale features are clearly at play (homopolar defects, typical intermediate range order) and these seem to bring the location of the stiffness transitions to lower compositions ($x = 30\%$ As) thus allowing us to reconsider the estimate ($x = 40\%$) usually computed from the simple condition [1] $\bar{r} = 2.4$. In fact, it is the first time that nonmonotonic trends in commonly calculated structural and dynamic properties from molecular simulations can be connected with experimental signatures of rigidity transitions and the intermediate phase. In this respect, the established relationship goes well beyond the

basic information extracted from constraint counting algorithms [1].

First principles molecular dynamics simulations [15,16] were performed on As_xSe_{1-x} systems consisting of $N = 200$ atoms at five different compositions (20%, 25%, 30%, 35%, 40% As) with the number of atoms being given by $N_{As} = xN$ and $N_{Se} = (1 - x)N$. A periodically repeated cubic cell was used, whose size changes according to the compositionally dependent number density of the glass [14]. The electronic structure was described within density functional theory and evolved self-consistently during the motion using a generalized gradient approximation for the exchange and correlation parts of the total energy, according to Becke and Lee, Yang, and Parr, respectively, Ref. [17]. Valence electrons were treated explicitly, in conjunction with normconserving pseudopotentials to account for core-valence interactions [18]. The wave functions were expanded at the Γ point of the supercell and the energy cutoff was set at 20 Ry. For all compositions and temperatures, statistical averages in the liquid state were obtained over 25 ps of trajectory with a time step of $\Delta t = 0.12$ fs and a fictitious mass of 200 a.u. At 1200 K, three uncorrelated configurations separated by 5 ps have been selected to provide starting sets of coordinates for a quench ($\simeq 10$ K/ps) leading to the obtention of three independent structures of an amorphous system at $T = 300$ K.

We show in Fig. 1 the total structure factor $S_T(k)$ for amorphous $As_{20}Se_{80}$, $As_{35}Se_{65}$ and $As_{40}Se_{60}$, compared to experimental data [9,19] and previous modeling [20,21]. It appears that our $S_T(k)$ agrees over the whole range of wave vectors for the stoichiometric compound (40% As). The two main peaks at 2.2 Å^{-1} and 3.7 Å^{-1} are very well reproduced as well as the peaks at higher k. For the lower compositions (20% and 35%), the agreement with experimental data is even better. A decomposition into partial structure factors indicates that a FSDP is present in $S_{AsSe}(k)$, whereas $S_{SeSe}(k)$ mostly contributes to the principal peak at 2.2 Å.

In Fig. 2 the partial structure factor $S_{AsSe}(k)$ dominating the FSDP in $S_T(k)$ is reported for the five compositions. We use a Lorentzian fit in order to extract the position k_{FSDP} and width Δk_{FSDP} of the FSDP. Results for these two quantities (inset) show that the position k_{FSDP} decreases from 1.25 Å^{-1} to 1.17 Å^{-1} between 20% and 40% As. While k_{FSDP} remains nearly constant at low As content, it drops at the approximate boundary of the experimentally determined rigidity transition, found at 29% As [14]. The width of the FSDP (inset of Fig. 2) also exhibits an anomalous behavior with a minimum found at 30% As. As the position of the FSDP reflects some repetitive characteristic distance between structural units, results of Fig. 2 suggest that in the flexible phase ($x \simeq 20\%$, [14]) a typical length scale of distance $L = 7.7/k_{FSDP} = 6.17$ Å builds up for the As-Se correlations with decreasing As content [22]. Similarly, the broadening of the FSDP is indicative of a

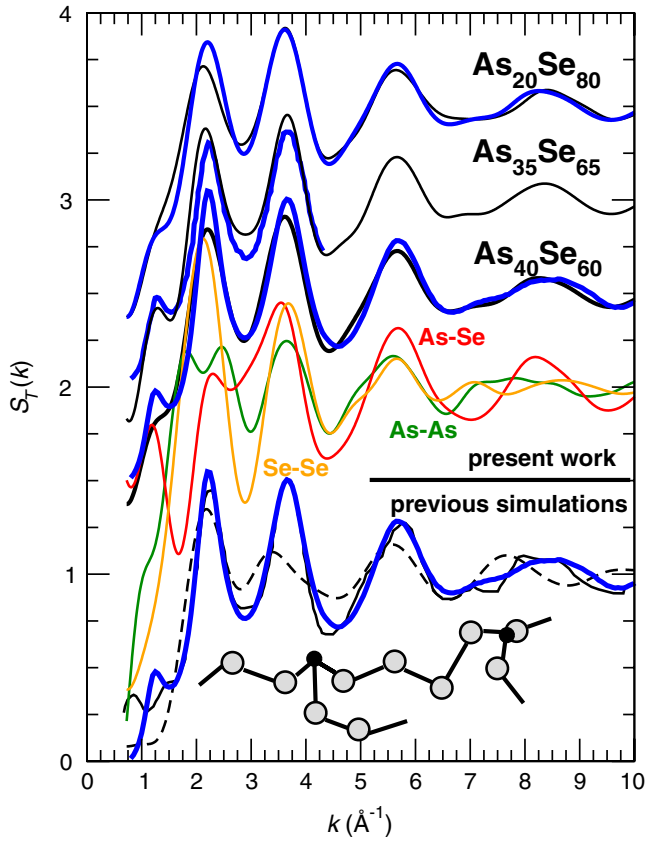

FIG. 1 (color online). Total simulated structure factor $S_T(k)$ of amorphous $As_{20}Se_{80}$, $As_{35}Se_{65}$, and $As_{40}Se_{60}$ (top, black solid lines) compared to previous simulations of $As_{40}Se_{60}$ (bottom) from Li and Drabold (solid line, [20]) and Mauro and Varshneya (broken line, [21]). All simulated functions are compared to experimental data (blue curves : $As_{40}Se_{60}$, [19]; other compositions, [9]). A decomposition into partial structure factors is shown for $As_{40}Se_{60}$: As-As (green), As-Se (red), Se-Se (orange). Bottom: a schematic view of the structure of a low modified As_xSe_{1-x} glass: $AsSe_{3/2}$ pyramids cross-link Se chains (see text for details).

coherence length, following the well-known Scherrer equation for microcrystals which connects the width of a Bragg peak with the average size of the microcrystals. This leads to the definition of a coherence length for ordering defined by $\xi = 7.7/\Delta k_{FSDP}$ which increases from $\xi = 4.30$ Å to 11.0 Å from $As_{20}Se_{80}$ to $As_{30}Se_{70}$, and then decreases with growing As content.

In real space, the predominant coordination motif in As_xSe_{1-x} glasses consists of cross-linking pyramidal $AsSe_{3/2}$ units into Se chains (see bottom of Fig. 1). However, close to 30% As, real space correlations are characterized by a threshold behavior, exemplified by the steep increase in the amount of As-As homopolar connections [Fig. 3(b)]. Indeed, while spanning the range of concentrations typical of the intermediate phase, drastic changes are found in the fraction n_{AsAs} of homopolar bonds which increases substantially [Fig. 3(b)] for $x \geq 30\%$.

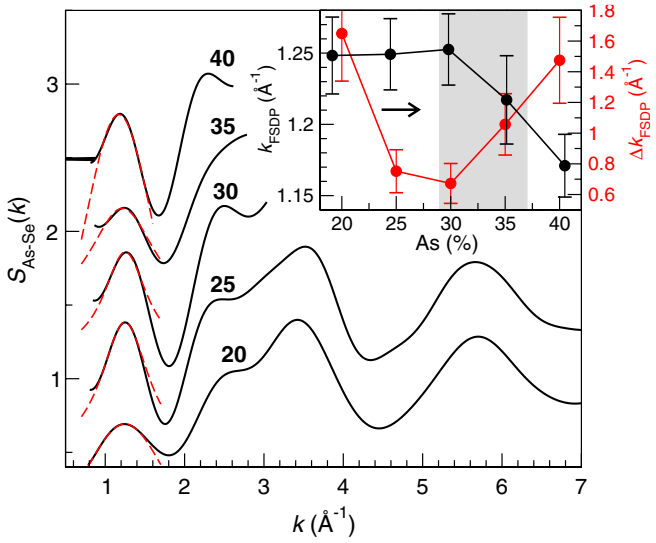

FIG. 2 (color online). Computed partial structure factor $S_{AsSe}(k)$ for the five amorphous compositions (from to 20% to 40% As) in amorphous As_xSe_{1-x}. The red broken curves are Lorentzian fits used to determine the position k_{FSDP} (inset) and width Δk_{FSDP} (inset, right axis) of the As-Se FSDP as a function of composition. The grey zone indicates the rigid intermediate phase, determined experimentally [14].

Conversely, fragments with pure Se-Se bonds display a continuous trend with As composition while the total fraction of homopolar bonds (Se-Se and As-As) displays a minimum value at the 30% As composition [inset of Fig. 3(b)]. In Fig. 3(a), As-As bonds are assumed to correspond to the prepeak at 2.60 Å in the pair distribution function g_{AsAs}, the prepeak at 2.37 Å in g_{SeSe} being

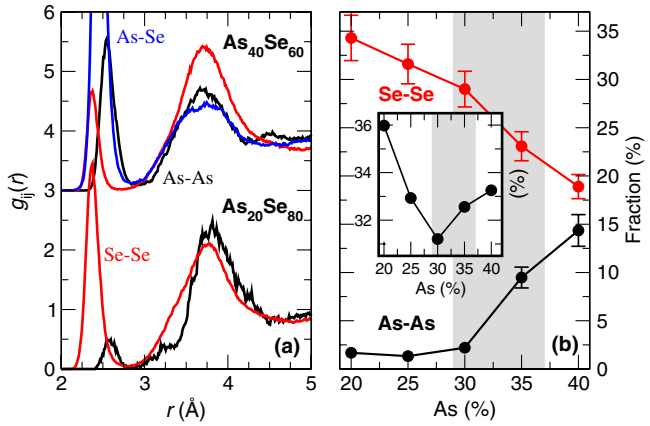

FIG. 3 (color online). (a) As-As (black line), As-Se (blue line), and Se-Se (red line) pair distribution function $g_{ij}(r)$ for two selected compositions in amorphous As_xSe_{1-x} ($x = 20$ and 40% As). For clarity, the As-Se pair is shown only for the 40% As system. (b) Computed fraction n_{AsAs} and n_{SeSe} of homopolar As-As and Se-Se bondings as a function of As composition. The grey zone indicates the rigid intermediate phase, determined experimentally [14]. The inset represents the total fraction of homopolar bonds as a function of composition.

associated with Se-Se homopolar bonds, i.e., the bond length of the base selenium glass [23]. Such trends can also be extracted qualitatively from the height of the prepeak in $g_{AsAs}(r)$ when moving from $As_{20}Se_{80}$ to $As_{40}Se_{60}$ [Fig. 3(a)]. However, they are hardly detectable from the analysis of the total pair distribution function [19], the homopolar As-As prepeak being overwhelmed by the large intensity of the As-Se first peak at 2.48 Å [Fig. 3(a)]. The important growth of homopolar As bonding for $x > 30\%$ is an indication of the increase of stressed rigidity in the network backbone [24] which leads in different chalcogenides (and particularly in As_xSe_{1-x}) to nanoscale phase separation with the growth of ethylenelike structures containing one As-As bond, once $x > 35\%$ As. On the other hand, one remarks that the upper boundary of the experimental IP is not acknowledged from real space calculated properties.

An analysis of the nearest-neighbor coordinations [25] shows that twofold Se and threefold As (90%–95%) are predominant. Also, As and the Se-centered bond angles have maxima close to 98°, in line with the experimental estimate [26]. Coordination defects arise from fourfold As which represents 6%–9% for all compositions, whereas onefold (terminal) Se are observed in smaller amounts (4%–6%).

The thresholds or anomalies with a composition of reciprocal (k_{FSDP}, Δk_{FSDP}) and real space properties (n_{AsAs}) are correlated with diffusivity anomalies in the liquid state. By calculating the mean square displacement $\langle r^2(t)\rangle$ at different temperatures (2000 K, 1600 K, 1200 K, 800 K), a diffusion coefficient D_i ($i =$ As, Se) can be extracted in the long time limit via the Einstein relationship $D_i(i = \text{As, Se}) = \lim_{t\to\infty}\langle r^2(t)\rangle/6t$ [27]. When represented as a function of inverse temperature, both D_{As} and D_{Se} exhibit an Arrhenius behavior, with an activation energy E_A that is represented in Fig. 4 as a function of composition. This quantity features a minimum at 30%–35% As (0.29 and 0.34 eV for Se and As, respectively). Both species also display a diffusivity anomaly in the same compositional interval with a maximum of $D_{Se} = 0.72 \times 10^{-5}$ cm^2/s obtained at 35% As.

The present results (Figs. 2–4) highlight the fact that in a certain compositional interval found between roughly 30%–35% As, As-Se bonding is predominant favoring the formation of coherent microdomains extending over intermediate range order distances ($\simeq 10$ Å) as revealed by the FSDP. These domains can form due to the low activation barriers and the enhanced diffusion of the species involved. Therefore, a close link exists between unmistakable fingerprints of structural and dynamical properties in the vicinity and within the intermediate phase.

As an extension, since the system displays a clear minimum in the activation energy E_A for diffusion, it is possible to infer that the same minimum should be found in the corresponding E_A for viscous flow, because the two energy

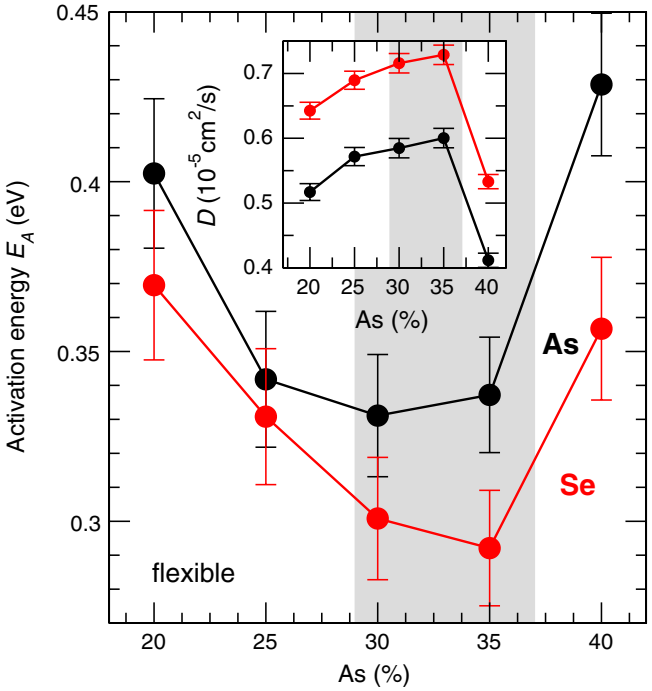

FIG. 4 (color online). Computed activation energy E_A for diffusion of As (black symbols) and Se (red symbols) as a function of As content in amorphous As_xSe_{1-x}. The insert shows the diffusion constant at 800 K. The grey zones indicate the location of the rigid IP, determined experimentally [14]. The flexible chalcogen-rich phase is marked.

barriers are usually close [28]. In the range $20 < x < 40\%$ As, the glass transition temperature increases from 100° C to 180° C [14] which allows us to compute the liquid fragility defined for an Arrhenius behavior by: $\mathcal{M} = E_A \ln_{10} 2/k_B T_g$. $\mathcal{M}$ takes a minimum value at 30% As with $\mathcal{M} = 22 \pm 1$, whereas $\mathcal{M} = 28 \pm 2$ and $\mathcal{M} = 25 \pm 1$ for 20% and 40% As, respectively. These results are in very good agreement with alternative determinations of the fragility minimum, either from viscosity measurements ($\mathcal{M} = 28$, [29]) or from calorimetric relaxation ($\mathcal{M} = 17$, [30]), displaying the minimum of $\mathcal{M}$ at the same composition of 30% As. From a simplified Kirkwood-Keating model of the glass transition [31], it has been found that chalcogenides satisfying the condition $n_c \simeq 3$ are strong glass-forming liquids (with a low $\mathcal{M}$) having an activation energy for viscosity or relaxation time that is minimum at this same $n_c \simeq 3$ value. This suggests that As-Se system must be stress-free at 30%–35% As. The latter conclusion is consistent with calorimetric and optical methods [14] determining the boundaries of the stress-free IP [32], located between 29% and 37% As. IP compositions have been found to be stress-free, and when the corresponding interval is represented (grey zone in Figs. 2–4), one realizes that most of the calculated structural and dynamic thresholds or anomalies are located within the IP compositions [14].

Taken together, these results reveal that reliable atomic-scale models are able to track effects of rigidity via the observation of structural and dynamical properties of glasses as a function of composition. These provide detailed information that goes clearly beyond simple topological schemes. For the specific As-Se system, a link is established between the structure in real and reciprocal space and the stiffness transition, including the intermediate phase. The widths of the FSDPs feature an anomalous behavior around 30%–35% As, lower than the value predicted from the condition $\bar{r} = 2.4$. The obtained maximum of the coherence length of ordering is associated with a minimum in the activation energy for diffusion in the pristine liquid phase. Turning to experiments and having established such correlations, one expects to observe anomalies across the stiffness transition not only from calorimetric [14] or optical [32] probes, but also from measurements sensitive to the atomic structure of these networks. In this context, neutron diffraction studies (via the isotopic substitution method) providing the partial structure factors across the required range of compositions are highly desirable.

The authors thank P. Boolchand, S. Le Roux, and P. Simon for useful discussions. Support from Agence Nationale de la Recherche (ANR) (Grant No. 09-BLAN-0109-01) is gratefully acknowledged. GENCI (Grand Equipement National de Calcul Intensif) is acknowledged for supercomputing access.

*To whom all correspondence should be addressed.
mmi@lptl.jussieu.fr

[1] J. C. Phillips, J. Non-Cryst. Solids **34**, 153 (1979); M. F. Thorpe, J. Non-Cryst. Solids **57**, 355 (1983).
[2] J. C. Maxwell, Philos. Mag. **27**, 294 (1864).
[3] X. W. Feng, W. J. Bresser, and P. Boolchand, Phys. Rev. Lett. **78**, 4422 (1997).
[4] D. I. Novita, P. Boolchand, M. Malki, and M. Micoulaut, Phys. Rev. Lett. **98**, 195501 (2007).
[5] A. Sartbaeva, S. A. Wells, M. M. J. Treacy, M. F. Thorpe, Nat. Mater. **5**, 962 (2006).
[6] P. Boolchand and W. J. Bresser, Nature (London) **410**, 1070 (2001).
[7] M. Micoulaut, C. Otjacques, J.-Y. Raty, and C. Bichara, Phys. Rev. B **81**, 174206 (2010).
[8] M. Micoulaut and M. Malki, Phys. Rev. Lett. **105**, 235504 (2010).
[9] E. Bychkov, C. J. Benmore, and D. L. Price, Phys. Rev. B **72**, 172107 (2005).
[10] M. T. M. Shatnawi, C. L. Farrow, P. Chen, P. Boolchand, A. Sartbaeva, M. F. Thorpe, and S. J. L. Billinge, Phys. Rev. B **77**, 094134 (2008).
[11] S. Hosokawa, Y. Wang, J.-F. Bérar, M. Sakurai, and W.-C. Pilgrim, J. Non-Cryst. Solids **326–327**, 394 (2003).
[12] D. Selvanathan, W. J. Bresser, and P. Boolchand, Phys. Rev. B **61**, 15 061 (2000).

[13] G. Chen, F. Inam, and D. Drabold, Appl. Phys. Lett. **97**, 131901 (2010).
[14] D. G. Georgiev, P. Boolchand, and M. Micoulaut, Phys. Rev. B **62**, R9228 (2000).
[15] R. Car and M. Parrinello, Phys. Rev. Lett. **55**, 2471 (1985).
[16] CPMD, Copyright IBM Corp. (1990–2012) and MPI für Festkörperforschung Stuttgart (1997–2001).
[17] A. D. Becke, Phys. Rev. A **38**, 3098 (1988); C. Lee, W. Yang, and R. G. Parr, Phys. Rev. B **37**, 785 (1988).
[18] N. Troullier and J. L. Martins, Phys. Rev. B **43**, 1993 (1991).
[19] S. Xin, J. Liu, and P. S. Salmon, Phys. Rev. B **78**, 064207 (2008).
[20] J. Li and D. A. Drabold, Phys. Rev. B **64**, 104206 (2001).
[21] J. C. Mauro and A. K. Varshneya, J. Non-Cryst. Solids **353**, 1226 (2007).
[22] We relate the position r of a peak in real space to the position k of a corresponding peak in Fourier space by using the relation $k \cdot r \approx 7.7$, which identifies the location of the first maximum of the spherical Bessel function $j_0(kr)$.
[23] A. V. Kolobov, H. Oyanagi, and K. Tanaka, Phys. Rev. B **55**, 726 (1997).
[24] S. Mamedov, D. G. Georgiev, T. Qu, and P. Boolchand, J. Phys. Condens. Matter **15**, S2397 (2003).
[25] M. Micoulaut, R. Vuilleumier, and C. Massobrio, Phys. Rev. B **79**, 214205 (2009); C. Massobrio, M. Micoulaut, and P. S. Salmon, Solid State Sci. **12**, 199 (2010); M. Bauchy, M. Micoulaut, M. Celino, S. Le Roux, M. Boero, and C. Massobrio, Phys. Rev. B **84**, 054201 (2011).
[26] S. Hosokawa, Y. Wang, W.-C. Pilgrim, J.-F. Bérar, S. Mamedov, and P. Boolchand, J. Non-Cryst. Solids **352**, 1517 (2006).
[27] C. Massobrio, A. Pasquarello, and R. Car, Phys. Rev. B **64**, 144205 (2001).
[28] M. Bauchy, B. Guillot, M. Micoulaut, and N. Sator, Chem. Geol., doi: 10.1016/j.chemgeo.2012.08.035 (2012).
[29] J. D. Musgraves, P. Wachtel, S. Novak, J. Wilkinson, and K. Richardson, J. Appl. Phys. **110**, 063503 (2011).
[30] S. Bhosle and P. Boolchand (private communication).
[31] M. Micoulaut, J. Phys. Condens. Matter **22**, 285101 (2010).
[32] F. Wang, S. Mamedov, P. Boolchand, B. Goodman, and M. Chandrasekhar, Phys. Rev. B **71**, 174201 (2005).